

## Data driven inverse stochastic models for fiber reinforced concrete

Ivica Kozar<sup>\*</sup>, Natalija Bede<sup>a</sup>, Anton Bogdanić<sup>b</sup> and Silvija Mrakovčić<sup>c</sup>

*Faculty of Civil Engineering, University of Rijeka, R. Matejčić 3, Rijeka, Croatia*

*(Received July 16, 2021, Revised August 30, 2021, Accepted October 11, 2021)*

**Abstract.** Fiber-reinforced concrete (FRC) is a composite material where small fibers made from steel or polypropylene or similar material are embedded into concrete matrix. In a material model each constituent should be adequately described, especially the interface between the matrix and fibers that is determined with the ‘bond-slip’ law. ‘Bond-slip’ law describes relation between the force in a fiber and its displacement. Bond-slip relation is usually obtained from tension laboratory experiments where a fiber is pulled out from a matrix (concrete) block. However, theoretically bond-slip relation could be determined from bending experiments since in bending the fibers in FRC get pulled-out from the concrete matrix. We have performed specially designed laboratory experiments of three-point beam bending with an intention of using experimental data for determination of material parameters. In addition, we have formulated simple layered model for description of the behavior of beams in the three-point bending test. It is not possible to use this ‘forward’ beam model for extraction of material parameters so an inverse model has been devised. This model is a basis for formulation of an inverse model that could be used for parameter extraction from laboratory tests. The key assumption in the developed inverse solution procedure is that some values in the formulation are known and comprised in the experimental data. The procedure includes measured data and its derivative, the formulation is nonlinear and solution is obtained from an iterative procedure. The proposed method is numerically validated in the example at the end of the paper and it is demonstrated that material parameters could be successfully recovered from measured data.

**Keywords:** experimental data inversed model; FBM; FRC; layered model; three-point beam bending

### 1. Introduction

In our work we are interested in extraction of material parameters from experimental data. However, the parameters of interest usually could not be measured directly. A special, inverse procedure has to be devised to extract non-measurable data. An inverse procedure can be formulated based on a ‘forward’ formulation that connects relevant parameters and available data.

Our analysis of fiber reinforced concrete (FRC) is based on the fiber bundle model (FBM). This is mostly due to stochastic parameters that are comprised in the FBM. One could use deterministic material models like Rukavina *et al.* (2019a, 2019b), Rukavina *et al.* (2019) but that does not explain

---

\*Corresponding author, Professor, E-mail: ivica.kozar@gradri.uniri.hr

<sup>a</sup>Assistant Professor, E-mail: natalija.bede@uniri.hr

<sup>b</sup>Ph.D. Student, E-mail: anton.bogdanic@gradri.uniri.hr

<sup>c</sup>Associate Professor, E-mail: silvija.mrakovcic@uniri.hr

variations in experimental data. In order to accommodate variations in experimental results we have adopted stochastic model that is based on the ‘fiber bundle representation’.

In FBM fibers are connected in parallel and have elastic and optionally, plastic properties. After reaching the peak load fiber either breaks down or degrades gradually, depending on the adopted model. Each fiber has slightly different material or geometric properties according to some probabilistic distribution, e.g., normal, uniform, cosine, etc. More details about FBM are given by Kožar *et al.* (2018). In our FBM the fiber peak tension load and the fiber area are described with the Gauss (normal) probability distribution. Each fiber has simple multi-linear load-displacement relation but observed as a bundle, they present a non-linear stochastic function. Behavior of each fiber is essential for material properties or bond-slip relation, as it is concluded by Kožar *et al.* (2019a). However, influence of one fiber is lost when the bundle is observed; bundle preserves initial material parameters and has rather permanent behavior regarding the resulting global force-displacement law. Based on that fact, FBM is generalized into a simpler material model based on an exponential formulation with two parameters, which is similar to the microplane material model (Ožbolt *et al.* 2001). It is this material model that is used to formulate a ‘forward’ model for three-point bending of beams mimicking the experimental three-point bending procedure. The main intention is to connect experimental data from laboratory to material parameters, especially regarding the fiber bond-slip relation.

Our ‘forward’ model in the simplest possible way relates local material properties and global sample behavior observed in a laboratory, e.g., load-displacement or bond-slip law. We have assumed a simple layered beam model that assumes axial forces in each layer but without any shear between the layers. Model is formulated from two balance equations: force and moment equilibrium in the cross section. The result is a system of two nonlinear algebraic equations that can be solved using Newton’s procedure. However, if one is interested in the fracture process, i.e., post-peak behavior, then there is more than one pair of solution and the procedure has to choose the one that is needed, the pre-peak or the post-peak solution.

Material parameters could not be extracted from such ‘forward’ model, which besides having multiple solutions, is a system of two nonlinear equations with parameters given implicitly. Iterative scheme for extraction of implicit parameters would be too cumbersome and sensitive. In order to extract relevant material parameters, we have formulated an inverse procedure based on the derivative of experimental data. In the novel inverse model, parameters are exposed and an iterative scheme, such as Newton scheme, could be used for the extraction of material parameters.

Once a forward model is known, we could try extracting initial parameters, i.e., global sample behavior has been known from the experiments and we would like to determine the local material properties. This inverse relation is described as an ‘inverse model’, or ‘inverse stochastic model’ in the case of stochastic material properties (e.g., Ibrahimbegović *et al.* 2020, Sarfaraz *et al.* 2018). In the latter case, we speak about estimation of the local material properties in a form of probability function properties, like mean value and variance of parameters. Inverse models for various FBMs are described by Kožar *et al.* (2019a), Kožar *et al.* (2020), Kožar *et al.* (2019b, c).

Our layered model is a basis for the formulation of an inverse model that could be used in parameter extraction from laboratory tests. The moment balance equation connects external moment on the beam and curvature of the cross section. This equation could be related to experimental results comprising external force and displacement. The main difficulty in formulation is contained in axial layer forces being multiplied by a distance of a layer. We have assumed that distances could be treated as a known function and have reformulated the balance equation. Mathematical formulation of our problem is expressed as an exponential function multiplied with square of a

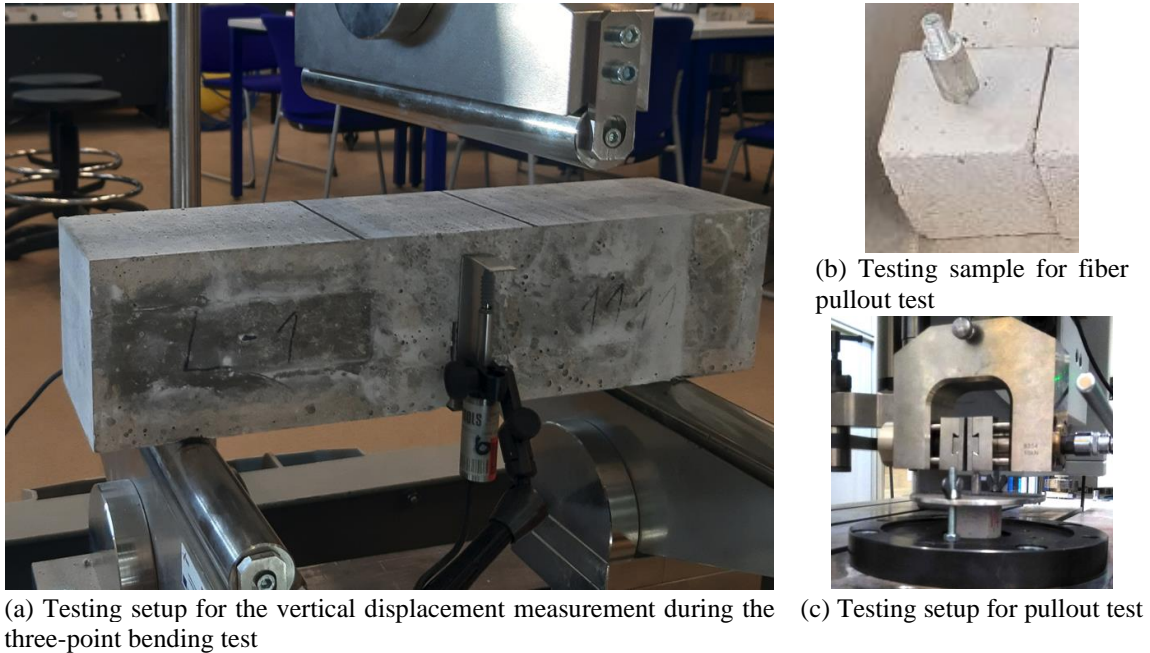


Fig. 1 Testing setups

known function. Material parameters are still implicitly present. This reformulated equation is further treated as a measurement equation, i.e., known, measured values are dependent from unknown parameters; this is the key assumption in the development of an inverse solution procedure. After we take the derivation of the equation and rearrange, parameters are exposed and an iterative scheme could be formulated. The procedure includes measured data and their derivative, the formulation is nonlinear and solution is obtained from an iterative procedure. There are multiple solutions to the parameter extraction problem and one has to choose the physically correct one. With small number of parameters, it can be done by inspection but we have provided another possibility, solution of the equation on the layer level. Layers have different solutions but all the layers comprise the correct solution, so the solution present in all the layers is the correct one; this is more practical for greater number of parameters.

In the present work, we are validating our novel inverse model for parameter extraction (in the sense described by Thacker 2004). Numerical example validates the novel iterative formulation that successfully recovered initial material parameters.

## 2. Laboratory testing

We have performed three-point bending laboratory tests with beams of different sizes and with different fibers. Fig. 1 presents several experimental setups for displacement measurement during loading. Fig. 1(a) presents the three-point bending test where we measure beam deflection and CMOD (Crack Mouth Opening Displacement), Fig. 1(b) is a specimen for the pullout test and Fig. 1(c) presents the pullout test as we conduct it. Experimental setup has to be meticulously prepared since measured data is the only source of information for the inverse model and parameter

estimation.

The main goal of our research is to relate the pullout and three-point bending tests. That would enable us to replace one type of test with the other and to achieve greater data redundancy that is important in parameter estimation and inverse modeling.

### 3. Material model

The simplest fiber bundle model consists of only elastic fibers with stochastic cross-section area that break at tension force ' $F_t$ '. The fiber bundle model relating the total force ' $F$ ' and displacement ' $\delta$ ' reads

$$F_{total} = \sum_{i_f=1}^{n_f} F_{i_f}(\delta, F_t, p(\mu A, \sigma A)) \quad (1)$$

Here, ' $p(\mu A, \sigma A)$ ' is (normal) probability distribution function with mean ' $\mu A$ ' and variance ' $\sigma A$ '. We could assume e.g., that variance ' $\sigma A$ ' is constant in the model so that ' $\mu A$ ', ' $\delta$ ' and ' $F_t$ ' remain the only parameters. Note that Kožar *et al.* (2019a) have presented the total force equation in the usual formulation with hidden stochastic properties although they are present in the model. This somewhat novel formulation for the FBM is required for better understanding of the inverse model (to be introduced later).

The problem is that the parameters we would like to estimate are within a function ' $p$ ' that is within a function ' $F_{i_f}$ '. Solution of such a problem could be very difficult or even impossible, depending on the actual formulation of functions.

It is important to somehow simplify the above function and we introduce the approximation ' $H(\mu A)$ ' of the probability function ' $p(\mu A)$ ' where ' $H(\mu A)$ ' is the histogram function from the known data. In that case, new force - displacement relation for a fiber bundle model reads

$$F_{total} = \sum_{i_b=1}^{n_{bin}} H(\mu A_{i_b}, \delta) \cdot F_{i_b}(\delta, F_t)$$

$$H(\mu A_{i_b}, \delta) = n_f \cdot \mu A \cdot p(\mu A, \sigma A, \delta) \quad (2)$$

This problem is much easier to solve, especially since ' $H(\mu A, \delta)$ ' could be pre-computed for assumed parameter value ' $\mu A$ ' and chosen values ' $\delta$ ' (points of the load-displacement curve where ' $\delta$ ' and ' $F_t$ ' are measured). This model could be made more elaborate by adding additional parameters, like plastic and unloading behavior of each fiber. The more elaborate model with 6 stochastic parameters proved to be successful in estimation of stochastic parameters from tension experiments where we were pulling-out fibers from a concrete block, (Kožar *et al.* 2018, Kožar *et al.* 2019a, Kožar *et al.* 2020).

It is evident from (Kožar *et al.* 2018, Kožar *et al.* 2019a, Kožar *et al.* 2020) that contribution of individual fibers results in the global force-displacement relation that represents the behavior of one specific volume of material. The global force-displacement relation could further be represented with one equation and contribution of individual fibers could be neglected. In our work, we chose microplane-like material model described with an exponential equation, (Kožar *et al.* 2019c, Kožar and Ožbolt 2010). Simplified microplane material model equation has only two parameters and reads

$$f(x, A, B) = A \cdot x \cdot \text{Exp}(-B \cdot x) \quad (3)$$

where ' $x$ ' is a displacement, in our case it could be the deflection ' $\delta$ ' or the CMOD, etc. Significance of parameters ' $A$ ' and ' $B$ ' is best seen from Fig. 2.

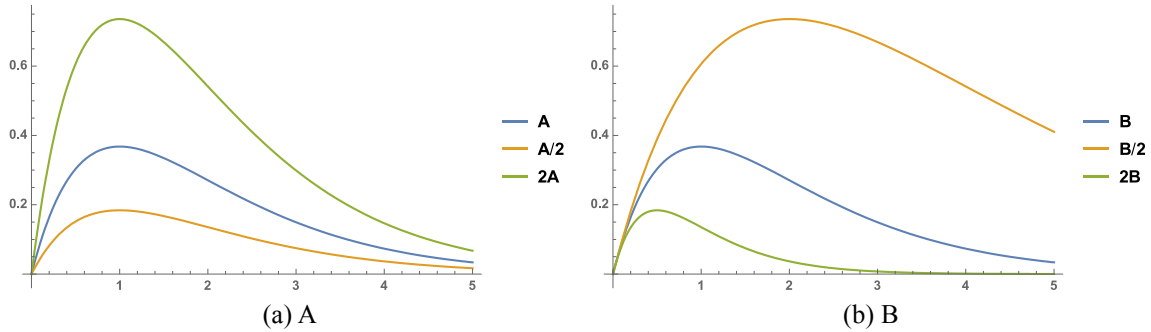


Fig. 2 Significance of parameters in the microplane material model

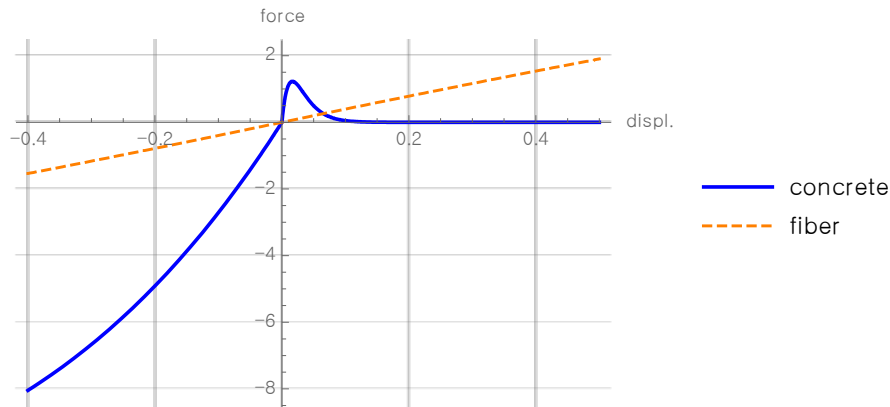


Fig. 3 Load-displacement diagram for the concrete matrix and for the fiber

Fig. 2 presents only the tension part of the load-displacement diagram and the compression part is similar but with different parameters. With only two parameters it is no possible to accommodate both curves, so we use different parameters for the compression behavior and do not have the common tangent at the zero displacement; this confirms to the fact that the tension and the compression moduli are different for concrete. The final equation is

$$f_c(x, A_c, A_t, B_c, B_t) = \begin{cases} A_c \text{Exp}(-B_c x) & \text{if } x < 0 \\ A_t \text{Exp}(-B_t x) & \text{if } x \geq 0 \end{cases} \quad (4)$$

Graphical representation is in Fig. 3

This exponential material model is further used for description of the all load - displacement relations.

### 3. Three-point beam bending model

A more complex problem emerged during experimentation with three-point bending of beams. Namely, we wanted to perform test of pull out of fibers in bending, not only in tension, since bending is the most common loading for fiber-reinforced beams. Moreover, direct tension experiments are very sensitive regarding the inclination, depth and the insertion procedure of fibers

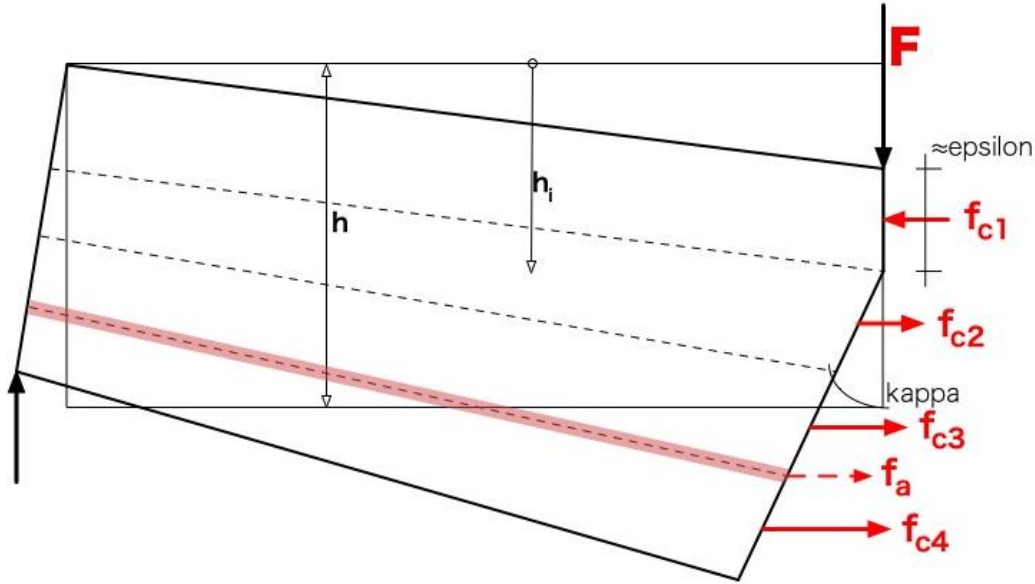


Fig. 4 Schematic representation of the layered beam model in three-point bending test

and we would prefer to replace them with bending experiments.

The first step in connecting experiments and material parameters is development of a model capable of reproducing experimental results up to the required degree. Numerical model for bending of beams assumed layered approach: beam is divided through height into layers where some layers could represent fibers and the other represent concrete. Each layer has a predefined force-displacement behavior based on the simplified fiber bundle model, as in the model above. Schematic representation of the layered model under the three-point bending test is given in Fig. 4.

The beam model is described with a system of two nonlinear equations (see Kožar *et al.* 2021 for layered model or Ibrahimbegović and Mejia-Nava (2021), Kožar *et al.* (2018) for a more complex model)

$$\begin{aligned} F(\varepsilon, \kappa) &= \Delta h \sum_i^{layers} f_c[(h_i - \varepsilon h) \cdot \tan \kappa] = F_{load} \\ M(\varepsilon, \kappa) &= \Delta h \sum_i^{layers} (h_i - \varepsilon h) \cdot f_c[(h_i - \varepsilon h) \cdot \tan \kappa] = M_{load} \end{aligned} \quad (5)$$

Here, ' $\Delta h$ ' is layer height (equal for all layers), ' $h_i$ ' is the position of layer ' $i$ ', ' $h$ ' is the total beam height, ' $(\varepsilon, \kappa)$ ' are the neutral axis position and the curvature, respectively, and ' $f_c$ ' is concrete force-displacement behavior in tension or compression. ' $F_{load}$ ' and ' $M_{load}$ ' represent external beam loading. Observe the additional function ' $(h_i - \varepsilon h)$ ' describing the layer position in the moment balance equation. Multiplication with this additional function prevents us from using the same approach as before. The above equations could be presented graphically where we see existence of multiple solutions of the nonlinear system of equations, Fig. 5.

Fig. 5 represents the solution path of the two equilibrium equations for same loading level: red is the force balance, dashed-blue is the moment balance; intersection of the two curves is the equilibrium position where both equations are satisfied for the given loading level. Fig. 5(a) represents the case of bending of the concrete beam without any fiber, i.e., all layer forces have the same load-displacement law, in which case we see two possible solutions for the same loading level.

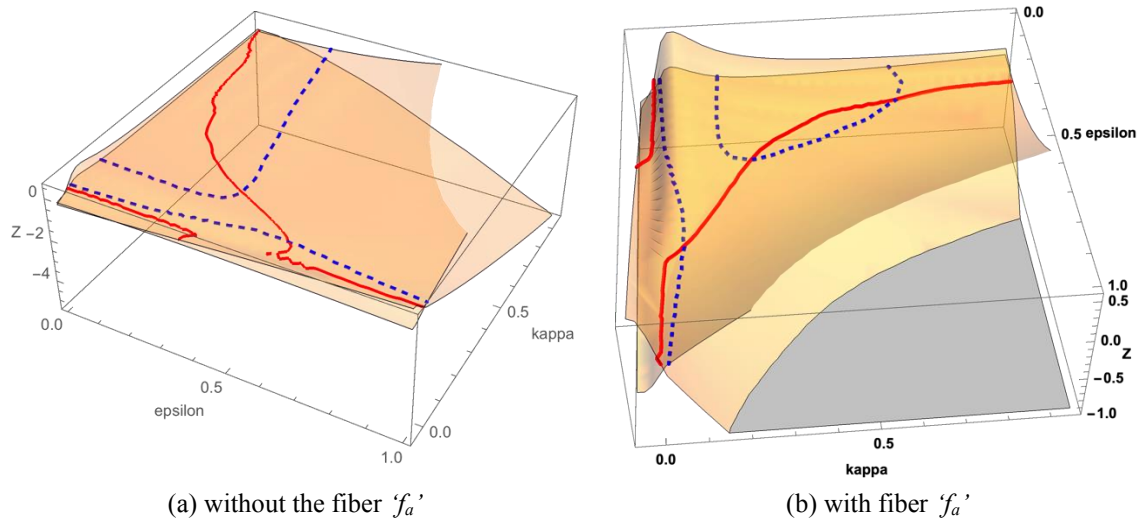


Fig. 5 Graphical representation of the equilibrium equations for beam in Fig. 3

On the other hand, Fig. 5(b) represents the case of bending of the beam with fibers, i.e., the layer with a fiber has different load-displacement law, in which case there are three possible solutions for the same loading level. From Fig. 5, it is evident that there are areas where the two equilibrium curves come close to each other making convergence of the numerical solution procedure difficult. Moreover, the number of solutions depends on the relation of the stiffness of concrete and reinforcement fibers.

Moreover, Fig. 5 shows the dependence between parameters of our layered beam model: the neutral axes position ' $\varepsilon$ ', the cross-section curvature ' $\kappa$ ' and the external loading ' $M$ '. The external loading is assumed to be known and the model results in ' $(\varepsilon, \kappa)$ ' values. The relation between the three-point bending tests is clear; during the test, we are recording the loading value, the vertical displacement and the CMOD (Crack Mouth Opening Displacement).

Note: both displacements are needed to uniquely identify the beam state because kinematic condition allows multiple CMOD for one vertical displacement and vice versa. Although we have not elaborated the exact relation, it is reasonable to assume that experimental results could be related to the moment-curvature curve ' $(m, \kappa)$ '; further on we will assume that experimental results are given as a ' $(m, \kappa)$ ' curve.

Fig. 6 graphically presents resulting curves ' $(\varepsilon, \kappa)$ ' and ' $(m, \kappa)$ ' for external moment in the interval  $m=[0, 0.04]$ .

#### 4. Inverse model

The purpose of our inverse model is to identify material parameters (as depicted in Fig. 2) from experimental results (assumed to be depicted as in Fig. 6(b)). In order to formulate the inverse model that would rely on measured values, we have to somehow relate experimental values and model parameters. When we combine material behavior Eq. (3) and moment balance Eq. (5) we obtain

$$M'(\varepsilon, \mathcal{E}) = \sum_i^{layer} A \cdot C_i(\mathcal{E})^2 \cdot \mathcal{E} \cdot \text{Exp}(-B \cdot C_i(\mathcal{E}) \cdot \mathcal{E}) \quad (6)$$

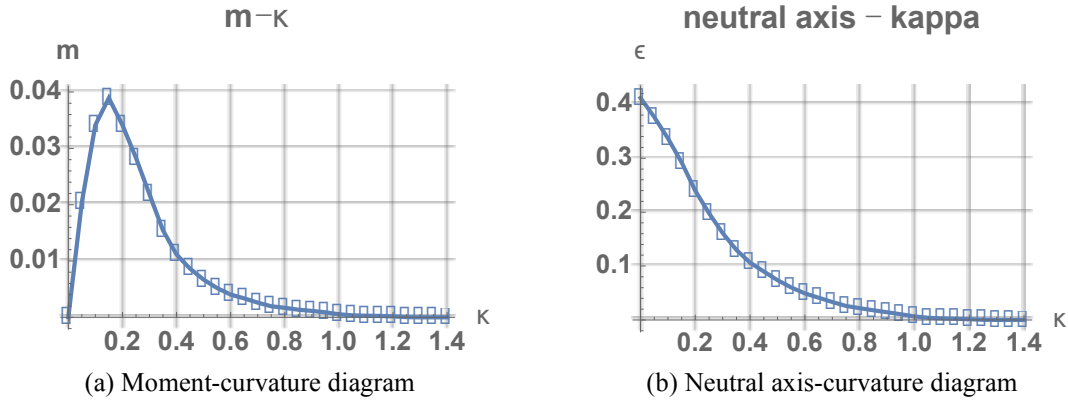


Fig. 6 Resulting curves

where

$$M'(\varepsilon, \Xi) = \frac{1}{\Delta h} M(\varepsilon, \Xi)$$

$$C_i(\Xi) = (h_i - \varepsilon h)$$

$$\Xi = \tan(\kappa)$$

We should write  $C_i(\Xi) = \text{function}(\Xi)$  because  $\varepsilon = \text{function}(\kappa)$  (see Fig. 6(a)). Moment values ' $M$ ' are recorded in the experiment but not for values of ' $\kappa$ '. ' $M$ ' values are taken at ' $m$ ' measuring points and, since ' $M$ ' is not a function of ' $\varepsilon$ ', we are introducing relation

$$\Xi \cong X_j.$$

$$M'(\varepsilon, \Xi) \cong Y_j \quad \text{at measuring points } j \in (1, \dots, m) \quad (7)$$

We note that ' $C_i$ ' could be tabulated for each layer in the model (note that parameters ' $A$ ' and ' $B$ ' remain equal for each layer), which enables us to use a data approach, i.e., we could assume some values are known from measurements. Equation for parameter identification now becomes (note that only one equation is sufficient for the identification procedure)

$$Y_j = \sum_i^{\text{layers}} A \cdot C_i^2 \cdot X_j \cdot \text{Exp}(-B \cdot C_i \cdot X_j) \quad (8)$$

Here ' $Y_j$ ' is the measured moment,  $X_j$  corresponds to the position where moment is measured and parameters ' $A$ ' and ' $B$ ' are to be determined (from measurements). Eq. (8) is a nonlinear equation regarding the parameter ' $B$ ' and in that form it is not suitable for determination of the parameter. An iterative scheme for calculation of the parameter ' $B$ ' has to be devised. In our case, the solution procedure is based on differentiation since it leads to disappearance of the parameter ' $A$ ', leaving only ' $B$ ' to in the formulation. The novel formulation requires calculation of derivatives of tabulated data, which could in practical realization be obtained through differentiation matrix applied on measured data. It is only here important to realize that  $C_i(\Xi) = \text{function}(X)$  so that the derivative  $C_i'(X_j)$  exists! Derivation of Eq. (8) over  $X_j$  results in

$$Y_j' = \sum_i \left[ \frac{Y_j}{X_j} + 2 \frac{Y_j}{C_i} C_i' - B Y_j C_i - B X_j Y_j C_i' \right] \quad (9)$$

Corresponding derivatives are obtained from measured (tabulated) data by derivation of an

interpolation function or by application of the derivation matrix. The only unknown in Eq. (9) is the parameter ‘ $B$ ’, which is calculated first using the least squares (in matrix form); parameter ‘ $A$ ’ is calculated later from Eq. (8). In order to calculate the parameter ‘ $B$ ’, Eq. (9) is reformulated as a measurement problem in matrix notation

$$Y_M = H_{M0}(B) - B \cdot H_{M1}(B) \tag{10}$$

where

$$Y_M = Y_j' - \sum_i \frac{Y_j}{X_j}$$

$$H_{M0}(B) = \sum_i \left[ 2 \frac{Y_j}{C_i} C_i' \right]$$

$$H_{M1}(B) = \sum_i \left[ -Y_j C_i - X_j Y_j C_i' \right]$$

Parameter ‘ $B$ ’ is iteratively calculated from Eq. (10), after that, parameter ‘ $A$ ’ is calculated from Eq. (8). For stable solution, it is important that the number of measure points is equal or greater than the number of layers.

### 5. Numerical example

This example represents a verification procedure for our inverse model under development (e.g., Thacker *et al.* 2004). In the example, we are trying to determine parameters for 14 layers ( $n=14$ ) and 20 measuring points ( $m=20$ ). Known functions ‘ $C_i$ ’ will be substituted with functions interpolated through random points (hopefully, this would confirm general validity of the procedure). During the interpolation, we have scaled the domain of interpolated functions so that it is in accordance with measured data (note the domain in Fig. 7(a) and Fig. 7(b) is different and in Fig. 7(b) and Fig. 8 it is the same). First, we establish the functions as presented in Fig. 7.

Measurements are simulated using Eq. (8) with parameters ‘ $A$ ’ and ‘ $B$ ’ set to ‘ $A=2.5$ ’ and ‘ $B=5.0$ ’, which we will try to recover using the inverse procedure.

The inverse procedure described with Eq. (10) represents the least square procedure whose solution is the optimum value of the parameter ‘ $B$ ’. It is a nonlinear equation with more than one solution and is solved using the Newton’s procedure. Plotting the residual, as in Fig. 9, we could see the existence of multiple solutions.

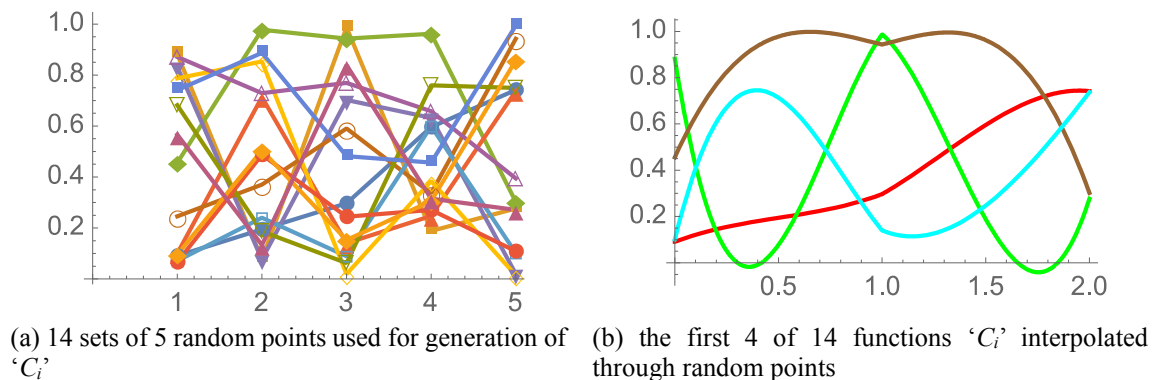


Fig. 7 Functions multiplying data

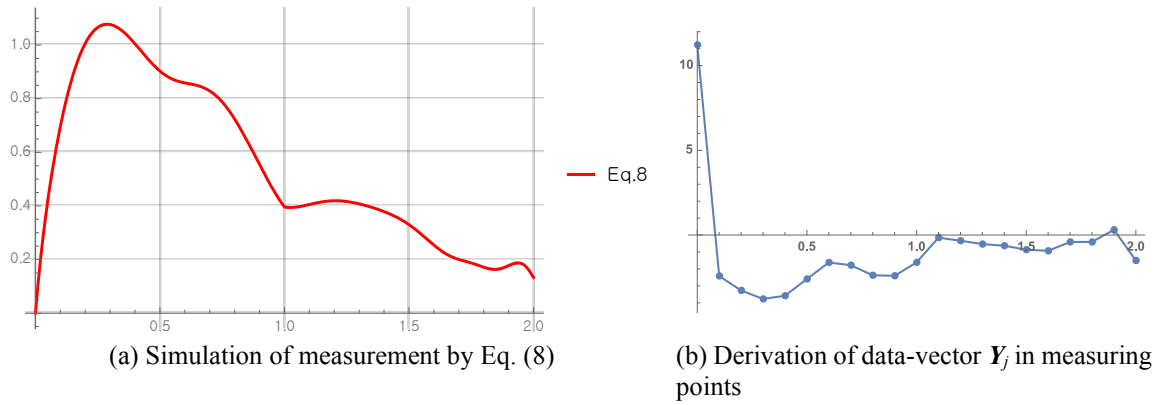


Fig. 8 Experimental data

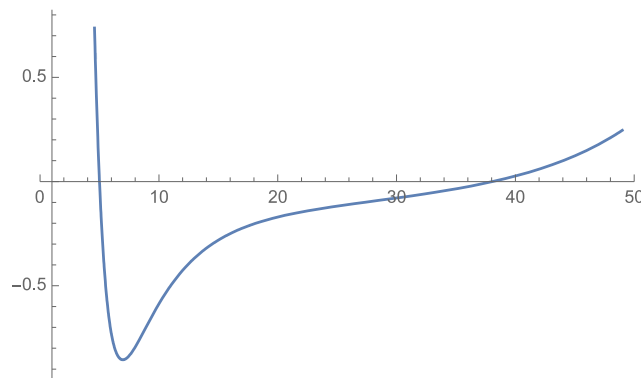


Fig 9 Parameter 'B' vs. the residual of Eq. (10)

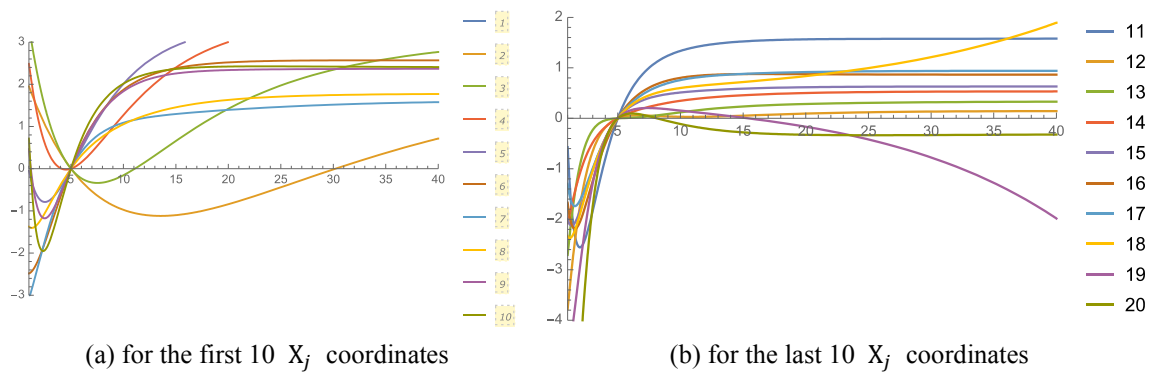


Fig. 10 Residues of Eq. (9) for values of parameter  $B \in [1.0 \dots 40.0]$

It is visible from Fig. 9 that there is more than one solution and care is needed in choosing the physically right one. However, there is an approach that could be helpful in selecting an appropriate solution: one could depict the residual for various measuring points of the Eq. (9); the solution that is comprised in all (or in the most) point residuals is the right one, as depicted in Fig. 10.

From Fig. 10 we could see that all out of 20  $X_j$  coordinates residue is zero for the same value

Table 1 Results for various measuring points 'r' for the initial value ' $B_0=2.0$ '

Meas.point 'r'	Iter.1	Iter.3	Iter.10	Iter.20	Iter.25	Iter.33	Iter.40
2	1.00000	4.78327	4.99998	5.00000	5.00000	5.00000	5.00000
7	1.00000	4.81377	4.99987	5.00000	5.00000	5.00000	5.00000
12	1.00000	3.52255	4.74245	4.96487	4.98656	4.99709	4.99937
18	1.00000	5.64509	5.00526	5.00001	5.00000	5.00000	5.00000

Table 2 Convergence of the Eq. (9)

Initial value	Iter.1	Iter.3	Iter.10	Iter.20	Iter.25	Iter.33	Iter.40
1.0	0.66667	0.964786	3.75145	4.27067	4.42349	4.61102	4.70863
2.0	1.33333	2.9739	4.3052	4.77562	4.86631	4.94016	4.97282
3.0	2.00000	3.92501	4.8798	4.99234	4.99804	4.99978	4.99997
6.0	4.00000	4.41325	5.11918	4.98655	5.00733	5.00098	4.99976

of the parameter ' $B$ ' (besides occasional zeros for other values of the parameter ' $B$ '). Now it is easy to find good initial value for Newton's procedure and the exact ' $B$ ' is calculated; the convergence of the Eq. (9) for several measuring points is given in Table 1.

The convergence of the Eq. (10), where we calculate the parameter ' $B$ ' for all the measuring points at once is somewhat different. Table 2 shows the convergence of Eq. (10) for various initial values of ' $B$ '.

We see that the parameter ' $B$ ' is successfully recovered and the parameter ' $A$ ' is calculated from Eq. (8); the result is  $A \in [2.479, 2.5008]$  for  $B \in [4.973, 5.001]$ . In the given intervals, error in the parameter ' $B$ ' is [0.54%, -0.02%] and error in the parameter ' $A$ ' is [0.85%, -0.03%] so there is no unacceptable amplification of the error.

## 5. Conclusions

Simple model of three-point beam bending is described with two nonlinear equations where material model for concrete is described with two-parameter exponential model. Model is compared with laboratory experimental results hoping that material parameters could be extracted from experimental data. Recovery of material parameters is not possible directly from the model equations so an inverse procedure has been derived. The novel inverse model based on the derivative of experimental data enabled successful recovery of material parameters.

Moreover, an inverse model based on integration of experimental data is under development.

## Acknowledgments

This work has been supported by Croatian Science Foundation through project HRZZ 7926 "Separation of parameter influence in engineering modeling and by the European Union through the European Regional Development Fund, Operational Programme "Competitiveness and Cohesion 2014-2020" of the Republic of Croatia, project "Protection of Structural Integrity in Energy and Transport" (ZaCjel, KK.01.1.1.04.0056), which is gratefully acknowledged.

## References

- Ibrahimbegović, A. and Mejia-Nava, R.A. (2021), "Heterogeneities and material-scales providing physically-based damping to replace Rayleigh damping for any structure size", *Couple. Syst. Mech.*, **10**, 201-216. <http://doi.org/10.12989/csm.2021.10.3.201>.
- Ibrahimbegović, A., Mathies, H.G. and Karavelić, E. (2020), "Reduced model of macro-scale stochastic plasticity identification by Bayesian inference in application to quasi-brittle failure of concrete", *Comput. Meth. Appl. Mech. Eng.*, **372**, 113428. <https://doi.org/10.1016/j.cma.2020.113428>.
- Kožar, I. and Ožbolt, J. (2010), "Some aspects of load-rate sensitivity in visco-elastic microplane model", *Comput. Concrete*, **7**(4) 317-329. <http://doi.org/10.12989/cac.2010.7.4.317>.
- Kožar, I., Bede, N., Mrakovčić, S. and Božić, Ž. (2021), "Layered model of crack growth in concrete beams in bending", *Procedia Struct. Integrit.*, **31**, 134-139. <https://doi.org/10.1016/j.prostr.2021.03.022>.
- Kožar, I., Ibrahimbegović, A. and Rukavina, T. (2018), "Material model for load rate sensitivity", *Couple. Syst. Mech.*, **7**, 141-216. <http://doi.org/10.12989/csm.2018.7.2.141>.
- Kožar, I., Torić Malić, N. and Rukavina, T. (2018), "Inverse model for pullout determination of steel fibers", *Couple. Syst. Mech.*, **7**, 197-209. <http://doi.org/10.12989/csm.2018.7.2.197>.
- Kožar, I., Torić Malić, N., Mrakovčić, S. and Simonetti, D. (2019b), "Combining deterministic and stochastic parameter estimation for fiber reinforced concrete modeling", *ECCOMAS MSF 2019*, Eds. A. Ibrahimbegovic, S. Dolarević, E. Džaferović, M. Hrasnica, I. Bjelonja, M. Zlatar, K. Hanjalić, Sarajevo, Bosnia and Hercegovina, September.
- Kožar, I., Torić Malić, N., Mrakovčić, S. and Simonetti, D. (2019c), "Parameter estimation in fiber reinforced concrete", *Proceedings of the International Conference on Sustainable Materials, Systems and Structures (SMSS2019)*, Eds. I. Gabrijel, C. Grosse, M. Skazlić, Rovinj, Croatia, April.
- Kožar, I., Torić Malić, N., Simonetti, D. and Božić, Ž. (2020), "Stochastic properties of bond-slip parameters at fibre pull-out", *Eng. Fail. Anal.*, **111**, 104478. <https://doi.org/10.1016/j.engfailanal.2020.104478>.
- Kožar, I., Torić Malić, N., Smolčić, Ž. and Simonetti, D. (2019a), "Bond-slip parameter estimation in fibre reinforced concrete at failure using inverse stochastic model", *Eng. Fail. Anal.*, **104**, 84-95. <https://doi.org/10.1016/j.engfailanal.2019.05.019>.
- Ožbolt, J., Li, Y.J. and Kožar, I. (2001), "Microplane model for concrete with relaxed kinematic constraint", *Int. J. Solid. Struct.*, **38**(16), 2683-2711. [https://doi.org/10.1016/S0020-7683\(00\)00177-3](https://doi.org/10.1016/S0020-7683(00)00177-3).
- Rukavina, I., Ibrahimbegovic, A., Do, X.N. and Markovic, D. (2019), "ED-FEM multi-scale computation procedure for localized failure", *Couple. Syst. Mech.*, **8**, 111-127. <https://doi.org/10.12989/csm.2019.8.2.111>.
- Rukavina, T., Ibrahimbegović, A. and Kožar, I. (2019a), "Fiber-reinforced brittle material fracture models capable of capturing a complete set of failure modes including fiber pull- out", *Comput. Meth. Appl. Mech. Eng.*, **355**, 157-192. <https://doi.org/10.1016/j.cma.2019.05.054>.
- Rukavina, T., Ibrahimbegović, A. and Kožar, I. (2019b), "Multi-scale representation of plastic deformation in fiber-reinforced materials: application to reinforced concrete", *Latin Am. J. Solid. Struct.*, **25**, 1-11. <https://doi.org/10.1590/1679-78255341>.
- Sarfaraz, S.M., Rosic, B.V, Matthies, H.G. and Ibrahimbegovic, A. (2018), "Stochastic upscaling via linear bayesian updating", *Couple. Syst. Mech.*, **7**, 211-231. <https://doi.org/10.12989/csm.2018.7.2.211>.
- Thacker, B.H., Doebbling, S.W., Hemez, F.M., Anderson, M.C., Pepin, J.E. and Rodriguez, E.A. (2004), "Concepts of model verification and validation", Los Alamos National Laboratory, LA-14167-MS. <https://doi.org/10.2172/835920>.